Glyceryl behenate-based solid lipid nanoparticles as a carrier of haloperidol for nose to brain delivery: formulation development, *in-vitro*, and *in-vivo evaluation*

Mohd Yasir*[1], Iti Chauhan[2], Ameeduzzafar Zafar[3] Madhu Verma[2],
Nabil K Alruwaili[3], K. M Noorulla[1], Alok Pratap Singh[4], Abdurrazak Jemal Tura[1]

[1]Department of Pharmacy, College of Health Sciences, Arsi University, Asella 396, Ethiopia,
[2]Department of Pharmaceutics, I.T.S College of Pharmacy, Muradnagar 201206, Ghaziabad,UP India,
[3]Department of Pharmaceutics, College of Pharmacy, Jouf University, Sakaka 72341, Al-Jouf, Saudi
Arabia, [4]SRM Modinagar College of Pharmacy SRMIST, Modinagar 201204, Ghaziabad, UP, India

This study was aimed to develop the haloperidol (HPL) loaded solid lipid nanoparticles (SLNs) for brain targeting through the intranasal route. SLNs were fabricated by the emulsification diffusion technique using glyceryl behenate as lipid and tween 80 as a surfactant. SLNs were evaluated for particle size, zeta potential, structure, entrapment efficiency, solid state characterization by differential scanning calorimetry (DSC), and *in-vitro* release. *In-vivo* biological evaluation was performed on albino Wistar rats for the determination of pharmacokinetic as well as brain targeting parameters. Particle size, PDI, zeta potential, and entrapment efficiency of optimized formulation (HPL-SLNs 6) were found to be 103±09 nm, 0.190±0.029, -23.5±1.07 mV, and 79.46±1.97% respectively. *In-vitro* drug release studies exhibited that 87.21± 3.63% of the entrapped drug was released from the SLNs within 24 h. DSC curves confirmed that during entrapment in SLNs, the drug was solubilized in the lipid matrix and converted into the amorphous form. Enhanced HPL targeting to the brain was observed from HPL-SLNs as compared to HPL-Sol when administered intranasally. The value of AUC 0-∞ in the brain for HPL-SLNs i.n. was found to be nearly 2.7 times higher than that of HPL-Sol i.v., whereas 3.66 times superior to HPL-Sol administered i.n. Stability studies revealed that the formulation remains unchanged when stored at 4±2 °C (refrigerator) and 25±2 °C /60 ±5% RH up to six months. Finally, it could be concluded that SLN is a suitable carrier for HPL with enhanced brain targeting through i.n administration, as compared to the HPL-Sol, administered i.n. and i.v.

Keywords: Biodistribution. Brain targeting. Haloperidol. Nose to brain delivery. Solid lipid nanoparticles. Pharmacokinetic.

INTRODUCTION

Haloperidol (HPL), which chemically belongs to the butyrophenone group, is an antipsychotic drug. It acts as a dopamine inverse agonist and blocks D2 dopamine receptors in the brain. Chemically, it is known as 4-(4-chlorophenyl)-1-[4-(4-fluorophenyl)-4-oxobutyl]-4-piperidinol] with a molecular weight of 375.86 g/mol and log P = 3.36 (Yasir, Sara, 2014). The major application of the drug is to treat certain psychiatric disorders like schizophrenia, manic states, medicament induced psychosis, and neurological disorders with hyperkinesias (Settle, Ayd, 1983). It is also useful to treat extreme behavior problems in children and to ease the symptoms of Tourette's syndrome (Forsman, 1976). Peak concentrations are achieved in 2 to 6 h after oral administration and the therapeutic range varies according to the pathological situation, but overall, positive effects are obtained for plasma concentrations between 1 and 17 µg/L. A major concern of HPL is the first-pass metabolism after oral delivery resulting in the reduction of bioavailability of

*Correspondence: M. Yasir. Department of Pharmacy. College of Health Sciences. Arsi University, Asella, Ethiopia. Phone: +251-904748369. E-mail: mohdyasir31@gmail.com. ORCID: https://orcid.org/0000-0001-9742-1482.

drug and hence only a small portion of the drug can reach to the brain by systemic blood (Chang, *et al.,* 1992). Moreover, HPL exhibits high plasma protein binding (90%) that further amplifies the bioavailability issue (Brincat, Macleod, 2004). Furthermore, certain clinical complications are associated with high systemic concentration which include respiratory disturbance (bronchospasm and increased depth of respiration), dermatological reactions (maculopapular and acneiform skin reactions), nausea, vomiting, and musculoskeletal disorder ((Budhian, Siegel, Winey, 2007). It may also induce a rare idiosyncratic reaction known as "neuroleptic malignant syndrome" which leads to severe symptoms such as hyperthermia, muscle rigidity, altered consciousness, hypertension, rhabdomyolysis, tachypnea, and tachycardia (Jann, Kennedy, 2016).

Solid lipid nanoparticles (SLNs) are colloidal particles of nano size (50-1000 nm). The drug may be either adsorbed or encapsulated in a lipid core matrix utilizing lipids of decent biological compatibility that are easily degradable, and inherit low toxicity (Wang *et al.,* 2019). Both, hydrophilic as well as lipophilic drug(s), are encapsulated in biocompatible lipid core consisting of either single lipid or combination of lipids, like compritol 888 ATO, precirol ATO 5, glyceryl monostearate, palmitic acid, stearic acid, etc, and stabilized by surfactant which is present at the outer shell. SLNs have been recognized as superior and alternative colloidal carriers over conventional ones such as polymer nanoparticles, liposomes, nanoemulsions, and microemulsions (Basha *et al.,* 2021; Patel *et al.,* 2014; Schwarz *et al.,* 1994). In comparison to others, the manufacturing processes of SLNs are also advantageous, because of less chance of residual contamination, employment of basic equipment, and ease in scale-up (Fricker *et al.,* 2010). SLNs offer other advantages like drug targeting, controlled drug delivery, increased bioavailability, and thus, reduced dose and side effects, etc (Schwarz *et al.,* 1994).

The brain is a sophisticated organ of the body and the blood-brain barrier (BBB) presents an obstacle to the transport of exogenous substances into the brain (Brasnjevic *et al.,* 2009). Thus, various approaches like drug manipulation, BBB disruption, and alteration in the route of administration like the application of intranasal route (olfactory pathways) are feasible for the targeting of drugs to the brain (Wong, Wu, Bendayan, 2012).

The intranasal route is a non-invasive approach and is supposed to bypass the BBB and reduce the systemic exposure and thus systemic side effects associated with the drug. Drug after intranasal administration reaches the olfactory epithelium region of the nasal mucosa that acts as a gateway for substances entering the CNS due to the neural connection between the nasal mucosa and the brain (Yasir *et al.,* 2018).

Thus, the study was aimed to develop haloperidol-loaded solid lipid nanoparticles (HPL-SLNs) for brain targeting, through the intranasal route, using the emulsification diffusion technique. SLNs were characterized by employing particle size, polydispersity index (PDI), and zeta potential to select the optimized formulation. Structural analysis, differential scanning calorimetry (DSC), and *in-vitro* release study were performed on the optimized formulation (HPL-SLNs 6). Furthermore, *in-vivo* biological evaluations like pharmacokinetic, biodistribution, and brain targeting parameters study were performed on albino Wistar rats after intranasal administration of optimized HPL- SLNs and compared with HPL-Sol (solution) administered intranasally (i.n) and intravenously (i.v).

MATERIAL AND METHODS

Material

HPL was obtained from Vamsi Labs Ltd (Solapur, Maharashtra, India) as a gift sample. Glyceryl behenate (Compritol® 888 ATO) and Glyceryl palmitostearate (Precirol® ATO 5) were obtained from Gattefosse (Witten, Germany) as a gift sample. Stearic acid, palmitic acid, acetonitrile (ACN), triethylamine (TEA), *o*-phosphoric acid (o-PA) and tween 80 along with all the other chemicals were purchased from Sigma-Aldrich (New Delhi, India). All solvents like ACN, TEA, *o*-PA were HPLC grade while other solvents and chemicals used were of analytical grade. Deionized water was used for the preparation of SLNs and it was filtered through a 0.22 μm membrane filter before use.

Methods

Excipients selection

Encapsulation efficiency is amongst the most influential factors for SLNs. The solubility of the drug in solid lipid plays an important role in proper drug entrapment in SLNs. However, equilibrium solubility studies cannot be carried out in this case. Hence, we used a modified method to select a solid lipid possessing better solubilization potential for the drug (Shah *et al.,* 2007). Several lipids like glyceryl behenate, glyceryl palmitostearate, stearic acid, and palmitic acid were screened to check the solubility of HPL.

A small quantity of HPL (20 mg) was taken in a vial. The solid lipids were separately heated around 5 ^{0}C above their melting points. These lipid melts were gradually added in portions to the vial containing HPL with continuous stirring using a vortex mixer and the same temperature was maintained (above the melting point of lipid). The endpoint of the solubility was the formation of a clear, pale yellow solution of molten lipid (Trotta, Debenaradi, Caputo, 2003). The amount of molten lipid required to solubilize the HPL was noted visually.

Preparation of SLNs

Several trial experiments were performed to optimize various factors like drug to lipid ratio (1:3, 50 mg: 150 mg), surfactant concentration (Tween 80 2 % w/v), chloroform to ethanol ratio (1:1, 2.5% *v/v,* mixture act as a solvent for drug and lipid), homogenization time 30 min/3000 rpm, stirring time (2.5 h), stirring speed (2500 rpm) & sonication time (5 min) and their effect were observed on particle size and entrapment efficiency. Factors like drug to lipid ratio, surfactant concentration, and stirring speed were further optimized. All of the experiments were performed in triplicate and the averages were considered as the response. Table I displays the composition of various batches. Modified solvent emulsification diffusion technique was used for the preparation of HPL loaded SLNs as per the scheme given in figure 1 (Singh, Saraf, Saraf, 2012).
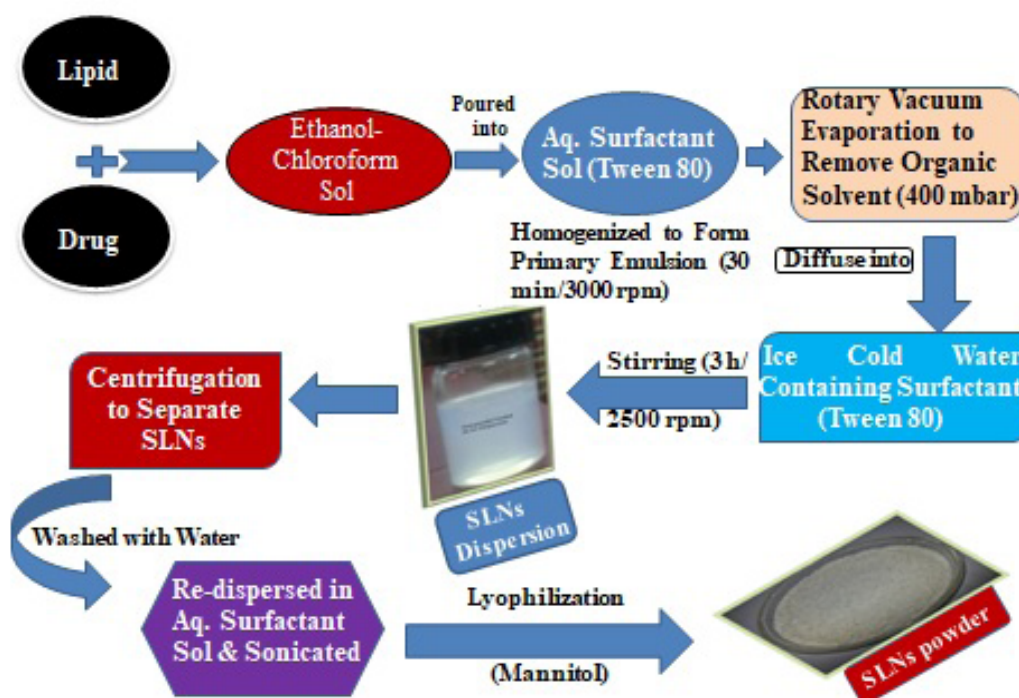
FIGURE 1 - Scheme for the preparation of HPL loaded SLNs.

Mohd Yasir, Iti Chauhan, Ameeduzzafar Zafar, Madhu Verma, Nabil K Alruwaili, K. M Noorulla, Alok Pratap Singh, Abdurrazak Jemal Tura

TABLE I - Composition of various batches of HPL-SLNs

Formulation code	Variables				
	Drug (mg)	Lipid (mg)	Surfactant % (w/v)	Stirring time (h)	Stirring Speed (rpm)
HPL-SLNs 1	50	100	2.0	2.5	2500
HPL-SLNs 2	50	150	2.0	2.5	2500
HPL-SLNs 3	50	200	2.0	2.5	2500
HPL-SLNs 4	50	150	2.5	2.5	2500
HPL-SLNs 5	50	150	2.0	3.0	2500
HPL-SLNs 6	50	150	2.50	3.0	2500
HPL-SLNs 7	50	150	2.5	3.0	3000

Characterization of HPL-SLNs

Particle size, zeta potential and structural study

Average particle size, polydispersity index (PDI), and zeta potential were measured by suitably diluting SLN dispersion. The analysis was performed at 25 °C with an angle of detection 90° (Jores, Mehnert, Drechsler, 2004) with help of photon correlation spectroscope (PCS; Zetasizer, HAS 3000; Malvern Instruments, Malvern, UK). The structure of drug-loaded SLNs was evaluated by Transmission electron microscope (TEM, Philips CM 10, Holland).

Determination of drug entrapment efficiency

A fixed quantity of HPL-SLNs dispersion (10 mL) was centrifuged (Remi Instruments, Pvt. Ltd, India) at 18,000 rpm for 20 min at 15 °C. Lipid matter was separated and the supernatant was analyzed spectrophotometrically at λ_{max} 247.5 nm (Shimadzu 1800, Japan) for determination of unencapsulated drug (Singh, Saraf, Saraf, 2012). Drug entrapment efficiency (%) was determined by using the following equations (1) (Alam *et al.*, 2015; Varshosaz, Tabbakhian, Mohammadi, 2010).

$$\text{Drug entrapment efficiency} \, (\%) = \frac{(W_t - W_s)}{(W_t)} \times 100$$

Where W_t is the total weight of drug used, W_s is the weight of the drug in the supernatant after centrifugation.

Differential scanning calorimetric analysis

The DSC curves of the drug, lipid, and optimized HPL-SLNs were recorded with a DSC (Pyris 6 DSC Perkin Elmer, CT, USA) under an inert atmosphere sustained by purging nitrogen (20 ml/min). A small amount (5 mg) of the sample was loaded into an aluminium pan and sealed tightly. An empty aluminium pan was used as a reference. Samples were heated at a heating rate of 10 °C/min over a temperature range between 40–220 °C and DSC curves were recorded (Chadha, Bhandari, 2014).

In-vitro drug release and release kinetics study

The dialysis bag diffusion technique was used to evaluate drug release (%) from HPL-SLNs. In this technique, a dialysis membrane (Himedia, molecular weight cut off 12000–14000 D) was used (Chen, Yang, Zhang, 2001). A measured quantity of HPL-SLNs containing HPL equivalent to 10 mg was taken in a dialysis bag and both ends of the bag were sealed. The sealed bag was then suspended in a beaker containing 100 mL of phosphate buffer pH 7.4 and stirred at a constant speed at 37±0.5 °C. Aliquots were withdrawn at predetermined time intervals up to 24 h from the receiver

compartment (beaker) and replaced with an equal volume of fresh medium to maintain sink condition. The samples were analyzed spectrophotometrically at λ_{max} of 247.5 nm (Shimadzu 1800, Japan). *In-vitro* release data was fitted to zero order, first order, & Higuchi release model and the correlation coefficient was determined from the graph for each model (Korsmeyer *et al.*, 1961; Higuchi *et al.*, 1961).

Stability studies

Stability studies were carried out to determine the influence of formulation additives on the drug stability and also to detect the physical stability of the prepared formulation at conditions of storage temperature and relative humidity (Soutto *et al.,* 2004).

The optimized HPL-SLNs formulation was subjected to stability studies as per the International Conference on Harmonization (ICH, 2003) guidelines and the studies were performed in triplicate. The storage conditions used for stability testing were 4±2 °C (refrigerator), 25±2 °C/60±5% RH, and 40±2 °C/75±5% in the stability chamber (Hicon instruments, N. Delhi). The sample was withdrawn after a period of 0, 1, 3, & 6 months and the effect of storage conditions was determined on particle size, PDI, zeta potential, & entrapment efficiency was determined.

In-vivo biological evaluation

In-vivo studies were performed on male albino Wistar rats (Adult/weighing 200-250 g). A protocol for animal studies was approved by the institutional animal ethical committee and the project number was 03.

In-vivo studies were performed for both HPL-Sol (positive control) & HPL loaded SLNs administered intranasally (i.n.) and HPL-Sol (positive control) administered intravenously (i.v.). For this purpose, rats were divided into three different groups (Haque *et al.*, 2014; Kumar *et al.*, 2008):

Group A: positive control for i.v. drug administration (HPL-Sol);

Group B: positive control for i.n. drug administration (HPL-Sol); and

Group C: i.n. formulation administration (HPL-SLNs).

Each group was divided into 6 subgroups (containing 6 animals in each on a time basis as, 0.5 h, 1 h, 2h, 4 h, 8 h, and 24h.

Procedure for drug administration and analysis: HPL-Sol (positive control), containing 0.179 mg (for rat weighing 200 g) of HPL (equivalent to 0.89 mg/kg body weight), was injected through the tail vein (10 µL) in one group of rats. Similarly, drug solution (HPL-Sol) and drug formulation (HPL-SLNs) containing 0.179 mg of HPL were administered in each nostril in the other two groups with the help of micropipette. Before the nasal administration of drug/ formulation, the rats were anesthetized by pentobarbital sodium (35–50 mg/kg, i.p) and held firmly from the back in a slanted position during nasal administration. Finally, each group rats were killed humanely by an overdose of pentobarbital sodium at different time intervals (0.5, 1, 2, 4, 8, and 24 h) and the blood was collected by cardiac puncture and stored in EDTA coated Eppendorf tubes (Haque *et al.*, 2014; Kumar *et al.,* 2008).

Simultaneously, the brain and other tissues (intestine, kidney, liver, lungs, and spleen) were removed, washed with normal saline and mechanically crushed. Various organs and blood were centrifuged at 4000 rpm for 20 min to separate the supernatant.

The supernatant (0.5 ml) of each sample was subjected to a liquid-liquid extraction technique using 100 µL loratadine (100 ng/mL) as an internal standard. Finally, the concentration of drug in each sample was determined by the HPLC technique using 100 mmol/L potassium dihydrogen phosphate–acetonitrile – triethylamine (10:90:0.1, *v/v/v*) as a mobile phase (Jain *et al.,* 2011).

Plasma concentration-time profiles of HPL after i.n. and i.v. delivery was evaluated by pharmacokinetic software (PK Functions for Microsoft Excel, Pharsight Corporation, Mountain View, CA, USA). Various pharmacokinetic parameters such as C_{max}, T_{max}, AUC_{0-t}, $AUC_{0-\infty}$, elimination rate constant (Ke), and mean residence time (MRT) were calculated. Statistical analysis was performed using Graph pad prism 5.0 (Graph pad software San Diego, CA). All results are expressed as mean ± SD. The difference among the groups was compared with the analysis of variance (ANOVA)

Mohd Yasir, Iti Chauhan, Ameeduzzafar Zafar, Madhu Verma, Nabil K Alruwaili, K. M Noorulla, Alok Pratap Singh, Abdurrazak Jemal Tura

followed by the Tukey-Kramer multiple comparison test. P-Value < 0.05 was considered statistically significant.

The extent of nose to brain delivery was evaluated by the following parameters (Abdelbary, Tadros, 2013).

1. The brain/blood ratio, at 0.5 h, following i.n. and i.v. administrations

2. The relative bioavailability (RB) percentages following the i.n. administration in the blood and brain. The relative bioavailability (%) of the intranasal HPL-SLNs formulation to intranasal HPL-Sol was determined according to the following equation (2).

$$RB\ (\%) = \frac{(AUC_{HP-SLNs\ (0-\infty)})i.\,n.}{(AUC_{HPsol\ (0-\infty)})i.\,n.}\ x100$$

3. The drug targeting index (DTI) can be described as the ratio of the AUC brain/AUC blood following i.n. administration to that following i.v. administration. The following equation (2) was used for the determination of DTI [17].

$$DTI = \frac{(AUC_{brain}\ /AUC_{blood})0 - 24\ i.\,n.}{(AUC_{brain}\ /AUC_{blood})0 - 24\ i.\,v.}$$

4. The drug targeting efficiency (DTE) percentage and the nose to brain direct transport percentage (DTP) [17]. The percent brain targeting efficiency (DTE %) and nose to brain direct transport percentage (DTP %) was calculated with the help of equation (3 & 4).

$$DTE\ (\%) = \frac{(AUC_{brain}\ /AUC_{blood})0 - 24\ i.\,n.}{(AUC_{brain}\ /AUC_{blood})0 - 24\ i.\,v.}\ x100$$

where $F = (AUC_{0-24,\ brain,\ i.v.}/AUC_{0-24,\ blood,\ i.v.}) \times AUC_{0-24,\ blood,\ i.n.}$, $AUC_{0-24,\ brain,\ i.n.}$ is the area under the curve of the brain following i.n. administration, $AUC_{0-24,\ brain,\ i.v.}$ is the area under the curve of the brain following i.v. administration, $AUC_{0-24\ blood,\ i.v.}$ is the area under the curve of blood following i.v. administration, $AUC_{0-24\ blood,\ i.n.}$ is the area under the curve of blood following i.n. administration.

RESULTS AND DISCUSSION

Characterization of solid lipid nanoparticles

Based on the results of various parameters like particle size, PDI, zeta potential, and entrapment efficiency, batch HPL-SLNs 6 was considered as an optimized formulation. For optimized formulation lipid (drug to lipid 1:3), surfactant (tween 80), stirring time and stirring speed were 150 mg, 2.5 % w/v, 3 h, and 2500 rpm respectively as depicted in table II. The optimized formulation was characterized by the following parameters:

TABLE II - Solubility of HPL (20 mg) in various lipids

Lipid name	Melting point of lipid (°C)	Amount of lipid required[#]
Glyceryl behenate	70	49.51± 1.83 (ns)
Glyceryl palmitostearate	56	55.34± 2.24*
Stearic acid	69	82.89± 2.10**
Palmitic acid	63	142.37± 2.06**

[#]Values are mean± SD, n=3, *P < 0.05 versus Glyceryl behenate, **P< 0.001 versus Glyceryl behenate. *P < 0.05 results are significant, **P < 0.001 results are highly significant, *P > 0.05 results are non-significant (ns)

Particle size, zeta potential and structural study

The particle size and zeta potential curve of the optimized formulation are shown in figure 2. The value of particle size, PDI and zeta potential was found to be 103±09 nm, 0.190±0.029, and -23.5±1.07mV respectively (Figure 2A and 2B). The low value of PDI indicated uniformity in the particle size. The structure of optimized SLNs was studied using TEM for the optimized formulation; a dense roughly spherical pattern was observed (Figure 2C). The results of particle size were in good agreement with the result established by TEM analysis.
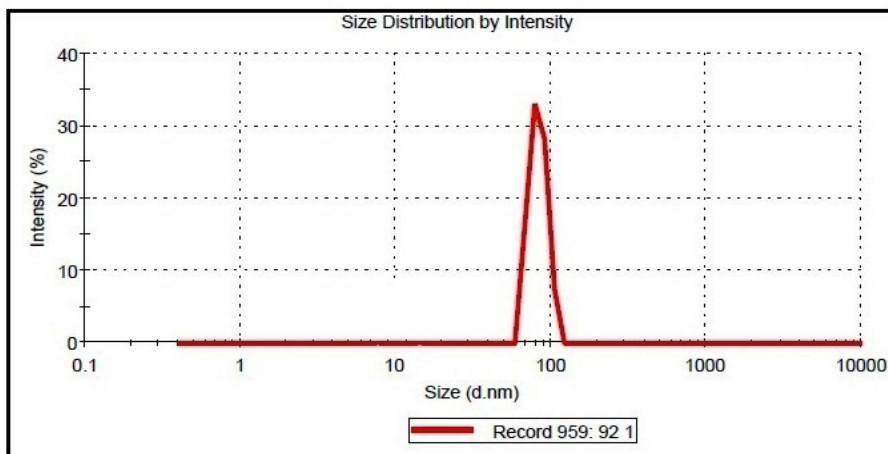
(A)
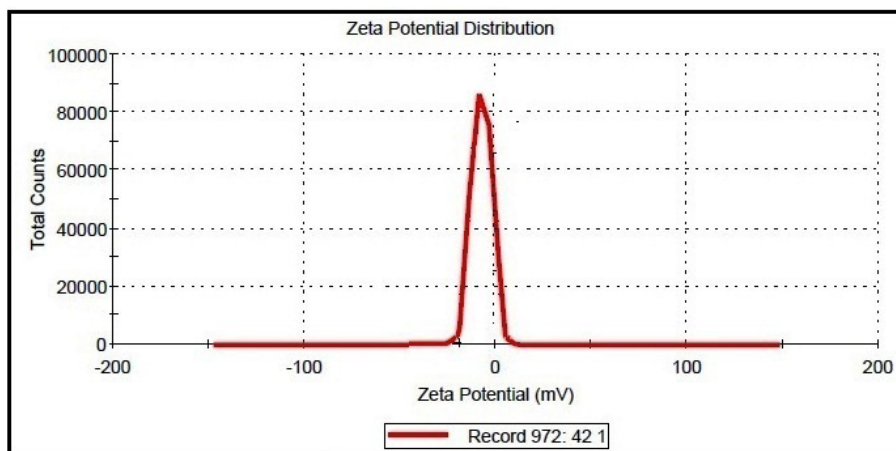
(B)
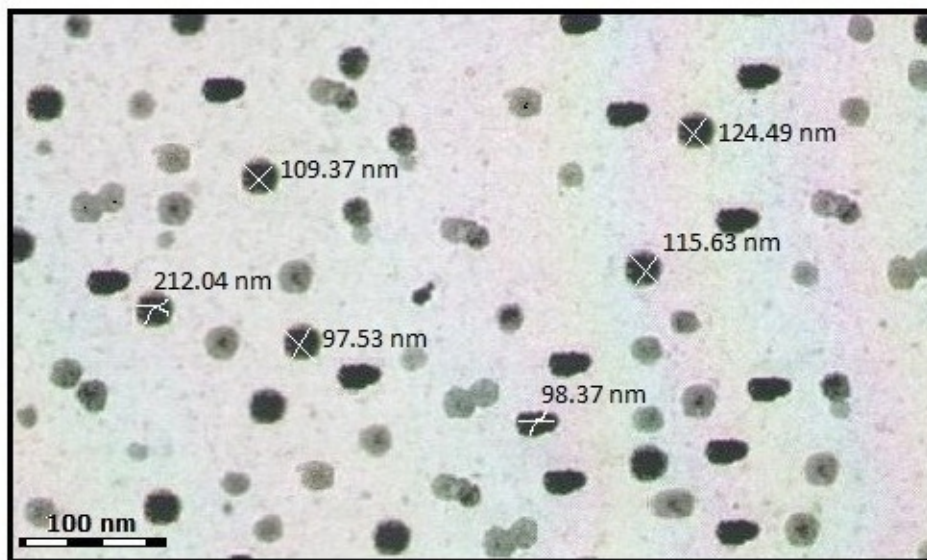
(C)

FIGURE 2 - Characteristic features of optimized formulation (A) Particle size (B) Zeta potential and (C) TEM image

Effect of lipid on particle size: At constant surfactant (2 %), particle size increases from 120±23nm HPL-SLNs 1 to 383±19 nm HPL-SLNs 3 with increasing the lipid amount (Table III) from 100 mg to 200 mg. This may occur due to the aggregation of particles on account of constant surfactant concentration, not enough to form a protective layer around each particle (Pandita *et al.,* 2009).

Effect of surfactant on particle size: At constant lipid amount, the particle size decreases with an increase in surfactant concentration. The particle size reduction is attributable to an increase in surface area during homogenization which was covered by available surfactant (Shah *et al.,* 2015). At constant lipid amount (150 mg), on increasing the surfactant concentration from 2 % to 2.5 %, the particle size decreased from 201±12 nm (HPL-SLNs 2) to 125±14 nm respectively (HPL-SLNs 4).

Entrapment efficiency study

The entrapment efficiency of optimized formulation (HPL-SLNs 6) was found to be 79.46± 1.98 %.

Effect of lipid on entrapment efficiency: The entrapment efficiency was found to be increased up to a certain limit on raising the amount of lipid, keeping surfactant concentration constant. This may be ascribed to the higher concentration of lipid which allows more space for entrapment of the drug and reduce the expulsion of the drug into the external phase. The entrapment efficiency of HPL-SLNs 3 formulation (74.08.±2.13% prepared with 200 mg) was more than HPL-SLNs 1 formulation (50.27±2.83% prepared with 100 mg) due to higher lipid content (Table III). The opposite results may be obtained on further increasing the lipid as a consequence of drug expulsion from the nanocarrier surface and the extent of drug solubility in the lipid (Pandita *et al.,* 2009).

Effect of surfactant on entrapment efficiency: At constant lipid amount, the surfactant concentration must be enough to prevent coalescence as it forms a coating layer around the nanoparticles. At this stage, a synergistic effect of surfactant was observed on entrapment efficiency (formulation HPL-SLNs 2, EE 71.95±1.26% with 2 % surfactant/ formulation HPL-SLNs 3, EE 78.18±1.02% with 2.5 % surfactant). Further increasing the surfactant, entrapment efficiency may decrease due to the formation of a micellar solution of the drug, accompanying enhanced drug solubility in the water phase (Shah *et al.,* 2015).

TABLE III - Formulation composition and characterization of various batches of HPL-SLNs

Formulation code	Variables					Responses			
	Drug (mg)	Lipid (mg)	Surfactant % (w/v)	Stirring time (h)	Stirring Speed (rpm)	Particle size (nm)	EE (%)	PDI	ZP (mV)
HPL-SLNs 1	50	100	2.00	2.5	2500	120±23	50.27± 2.83	0.219±0.025	-22.32±0.51
HPL-SLNs 2	50	150	2.00	2.5	2500	201±12	71.95± 1.26	0.312±0.029	-18.47±0.39
HPL-SLNs 3	50	200	2.00	2.5	2500	383±19	74.08.± 2.13	0.437±0.013	-15.82±0.85
HPL-SLNs 4	50	150	2.50	2.5	2500	125±14	78.18± 1.02	0.186± 0.009	-20.82±0.92

TABLE III - Formulation composition and characterization of various batches of HPL-SLNs

Formulation code	Variables						Responses		
	Drug (mg)	Lipid (mg)	Surfactant % (w/v)	Stirring time (h)	Stirring Speed (rpm)	Particle size (nm)	EE (%)	PDI	ZP (mV)
HPL-SLNs 5	50	150	2.00	3.0	2500	213±23	69.32± 2.58	0.283± 0.008	-20.97±0.72
HPL-SLNs 6	50	150	2.50	3.0	2500	103±09	79.46± 1.97	0.190±0.029	-23.5±1.07
HPL-SLNs 7	50	150	2.5	3.0	3000	112+13	77.64± 2.17	0.237± 0.009	-22.67±0.82

*Values are mean ± SD, n=3, EE= entrapment efficiency, PDI = polydispersity index, ZP= zeta potential

Differential scanning calorimetric analysis

The DSC curve of HPL (labelled 3A), glyceryl behenate (labelled 3B), lyophilized blank SLNs (labelled 3C), and HPL loaded SLNs (labelled 3D) are shown in figure 3. HPL showed a sharp endothermic peak at 151.25 °C (enthalpy = 186.36 J/g), and glyceryl behenate exhibited a specific endothermic peak at 73.36 °C (enthalpy =393.49 J/g) while lyophilized blank and lyophilized HPL loaded SLNs showed a glyceryl behenate endothermic peak little shifted to a lower temperature at 70.52 °C. The enthalpy of melting of lyophilized blank and lyophilized HPL loaded SLNs were found to be 73.29 J/g and 68.70 J/g respectively As shown in figure 3, the principal melting peak of HPL was absent in the DSC curve of SLNs as well as broadening of glyceryl behenate peak, emphasizing drug solubilization in the lipid matrix and its existence in the amorphous form. Moreover, the decrease in the melting point of glyceryl behenate might be attributed due to particle size reduction and a corresponding increase in the surface area. This leads to a decrease in melting enthalpy as compared to larger particulates which require more energy to overcome lattice forces (Bunjes, Unreh., 2007). The curve of lyophilized blank and lyophilized HPL loaded SLNs showed an extra endothermic peak at 154.5 °C. This peak might be due to the presence of mannitol (cryoprotectant) added during lyophilization. Similar findings were observed by Gidwani and Vyas (2016).
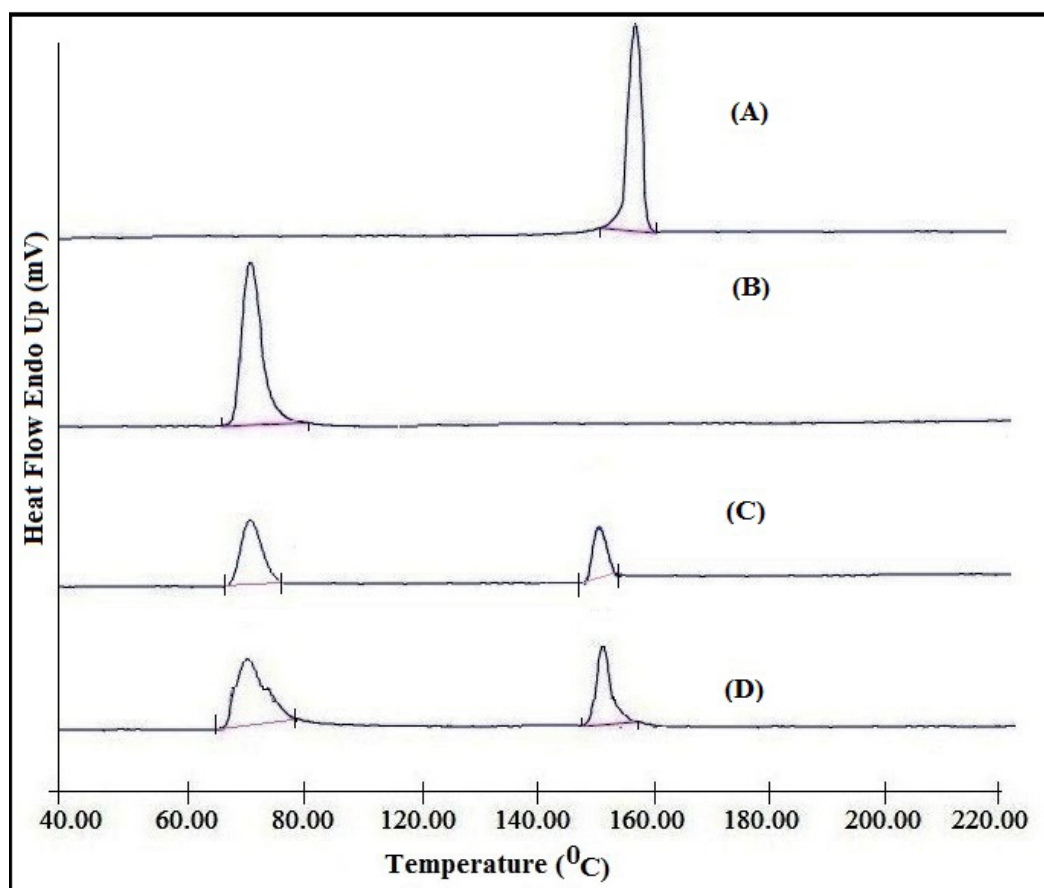
FIGURE 3 - DSC analysis of (A) HPL (B) Glyceryl behenate and (C) Blank SLNs (D) Optimized SLNs formulation

In-vitro *release of HPL from HPL-SLNs*

The comparative *in-vitro* release studies were performed between drug suspension (HPL-Sol) and optimized HPL-SLN (Figure 4).

A biphasic pattern consisting of an initial burst release, followed by a phase of slow- release was evident from the dissolution profile of optimized formulation. The early burst release may be due to the presence of free drug at the surface of lipid particles. The optimized HPL-SLNs showed an initial burst release of 21.33±3.53 %, whereas plain drug showed 68.17± 6.53 % drug release after 1 h. Thereafter, it showed sustained drug release with a maximum value of 87.21 ± 3.63 % in 24 h, while aqueous drug suspension displayed 97.72 ± 2.88% within 4 h. A significant difference ($P < 0.05$) was observed in drug release from drug suspension and SLNs after completion of 4 h study.
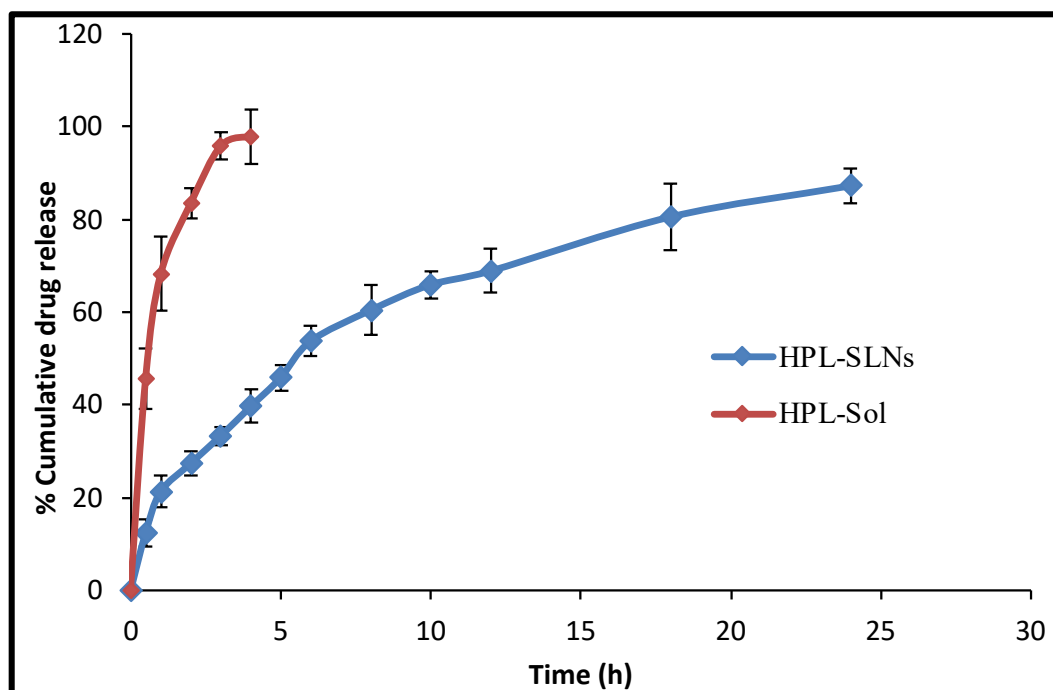
FIGURE 4 - Graph of *In-vitro* release study of optimized formulation.

Release kinetics of optimized formulation comply with the Higuchi's model with a correlation coefficient, $R^2 = 0.9961$. The value of Korsmeyer–Peppas release exponent "n" was found to be 0.782 indicating non-Fickian diffusion (anomalous transport) type of release mechanism, depicting that the drug release from lipid nanoparticles was controlled by more than one process i.e. diffusion and erosion.

Stability studies

Experimentation was carried out as per the ICH (2003) stability testing guidelines. For particle size, no significant (P<0.05) difference was observed when the optimized formulation was stored at 4± 2 °C (refrigerator) and 25±2 °C /60 ±5% RH up to six months, however, the particle size was increased significantly ($P < 0.001$) when the formulation was stored at 40±2 °C /75 ±5% RH due to aggregation. The average particle size after 6 months at 40±2 °C /75 ±5% RH was found to be 1369.63 ± 28.37 nm while the PDI was 0.727±0.096. Zeta potential plays an important role in the physical stability of nanoformulation. Like particle size, no significant alteration observed in

the zeta potential of optimized formulation when it was stored at 4±2 °C (refrigerator) and 25±2 °C /60 ±5% RH up to six months but a significant drop (P < 0.001) in zeta potential was observed at 40±2 °C /75 ±5% RH. This may be due to the fact that since, at high temperature & relative humidity, the outer surfactant coating gets dissolved leading to aggregation of lipid nanoparticles (Yasir *et al.,* 2018). The entrapment efficiency (%) was also reduced with time and temperature but no significant difference (P < 0.05) was observed.

In-Vivo Biological Evaluation

Pharmacokinetic and biodistribution studies were performed on Wistar albino rats.

Pharmacokinetic study

As shown in figure 5, the concentration of HPL in the brain after i.n. administration of HPL-SLNs was found to be significantly higher at all the time points as compared to both HPL-Sol i.n. and HPL-Sol i.v. (P <0.05). The HPL concentration in plasma after i.n. administration

of HPL-SLNs was found to be significantly lower at all the time points compared to HPL-Sol i.v. administration ($P<0.05$). The presence of the drug in plasma after HPL-SLNs intranasal administration is expected since i.n. route can also lead to systemic drug absorption (Jain, Nabar, Dandekar, 2010). Various pharmacokinetic parameters of HPL were observed and the lower value of Tmax for the brain (2 h) as against blood (4 h) may be associated with the preferential nose to brain transport following i.n. administration. A significantly ($P<0.05$) higher concentration of drug was found in the brain after the intranasal administration of HPL-SLNs (Cmax 123.74±9.24 (ng/ml)) as compared to HPL-Sol administered intranasally (Cmax 29.78±3.27 ng/ml) and intravenously (Cmax 32.65±6.83 ng/ml). As shown in table IV, the value of AUC0-∞ (626.27± 7.38 ng.h/mL) for HPL-SLNs administered intranasally was found to be significantly ($P<0.05$) higher than HPL-Sol (i.n. and i.v.). This may occur because of the direct transport of drug via the olfactory route by bypassing BBB. The value of AUC0-∞ in the brain for HPL-SLNs i.n. was found to be nearly 2.70 times higher than that of HPL-Sol i.v., whereas 3.66 times higher than HPL-Sol i.n.
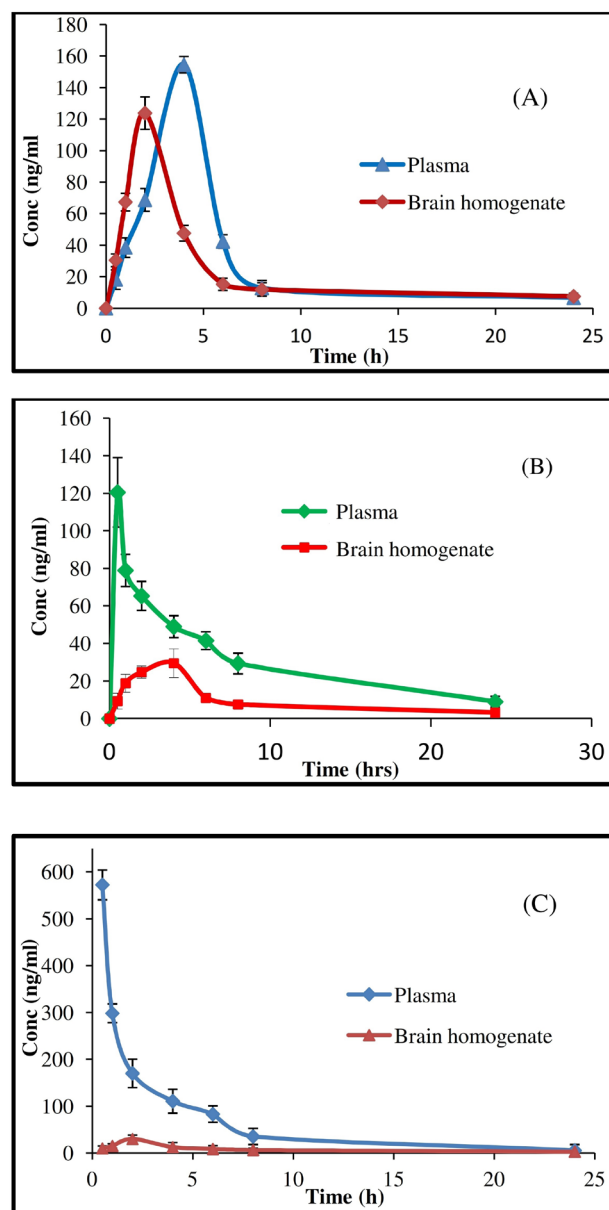
FIGURE 5 - Pharmacokinetic study of (A) HPL-SLN i.n. (B) HPL-Sol i.n. and (C) HPL-Sol i.v.

TABLE IV - Pharmacokinetic parameters of HPL i.n. brain and plasma after HPL-SLNs i.n., HPL-Sol i.n. and HPL-Sol i.v. administration to rats

P'kinetic parameters	Type of formulation/route of administration					
	HPL-SLNs i.n.*		HPL-Sol i.n.#		HPL-Sol i.v.	
	Brain	Plasma	Brain	Plasma	Brain	Plasma
C_{max}(ng/ml)	123.74±9.24	154.62±12.51	29.78±3.27	120.53±7.63	32.65±6.83	572.62±31.27
T_{max} (h)	2	4	4	0.5	2	<0.5
$AUC_{0-24\,h}$ (ng·h/ml)	544.86± 12.84	704.47± 21.01	129.78± 12.52	734.46± 25.73	198.54± 13.75	1533.95± 17.73
$AUC_{0-\infty}$ (ng·h/ml)	626.27± 7.38	783.45± 11.65	170.96± 16.43	824.85± 19.91	232.22± 17.91	1566.93± 35.38
$AUMC_{0-24\,h}$ (ng·h²/ml)	3299.38± 27.93	4194.72± 110.90	1603.06 ±99.63	5008± 97.42	1382.32± 47.63	6546.89± 285.93
$AUMC_{0-\infty}$ (ng·h²/ml)	6121.34± 23.57	7024.32± 51.62	3131.40 ±136.92	8090.67± 319.74	2985.41± 109.84	7502.12± 259.53
K_e (h⁻¹)	0.093± 0.001	0.08± 0.002	0.07 ±0.002	0.099 ±0.02	0.07 ±0.003	0.17 ±0.00
MRT (h)	9.777± 0.037	8.89± 0.02	11.55± 0.32	9.89± 0.13	12.86± 0.21	4.7± 0.06
RB (%)[a]	231.03± 15.84	94.98± 9.46				

Values are mean ± SD, *n*=6, [a] relative to i.n. HPL-Sol., *P < 0.05 versus HPL-Sol. i.n.,
*P < 0.05 versus HPL-Sol. i.v., #P< 0.05 versus HPL-Sol. i.v.

Brain targeting parameters study

The extent of the nose to brain delivery was evaluated by the following parameters:

(a) *Brain to blood ratio*: As shown in the table V, ratio of concentration of drug in the brain to blood, at 0.5 h, following intranasal and intravenous administrations, was determined. This value was found to be 1.66, 0.079, and 0.018 for HPL-SLNs i.n., HPL-Sol i.n and HPL-Sol i.v. respectively. The significantly higher brain/blood ratio of HPL-SLNs indicated the brain targeting potential of developed SLNs formulation. Similar findings were observed by Kumar *et al.* (2008).

(b) *Relative bioavailability*: Compared to HPL-Sol administered intranasally, the percent relative bioavailability of intranasal HPL-SLNs, in brain and blood were 366.30± 15.84 (3.66 fold) and 94.98± 9.46 respectively indicating enhancement in the bioavailability (P< 0.05) of HPL in the brain following the intranasal administration of HPL-SLNs (Table V). These findings are in line with Abdelbary, Tadros (2013).

(c) *Value of DTI, DTE (%) and DTP (%)*: Parameters like DTI, DTE (%), and DTP (%) indicate the percentage of the drug directly transported to the brain via the olfactory or trigeminal pathway. The value of DTI, DTE & DTP for HPL-SLNs administered intranasally was found to be 5.39, 539.31 % & 87.22%. While the value of DTI, DTE & DTP for HPL-Sol administered intranasally was found to be 2.33, 233.47 % & 56.17 % respectively (Table V). The DTI values >1 confirm the direct pathway from nose to brain (Yasir *et al.*, 2018). These findings are in line with

Jain *et al.* (2010) and Kanazawa *et al.* (2011) who found that micellar nanocarriers of zolmitriptan & coumarin increase the nose to brain uptake, via the olfactory region of the nasal cavity. Finally, it was concluded that the higher value of DTI, DTE (%), and DTP (%) suggest a better brain targeting potential of HPL-SLNs as compared to HPL-Sol administered intranasally. Similar findings have also been reported previously by Zhang *et al.* (2004)**.**

TABLE V - Results of Brain/Blood Ratio at 0.5 h, DTI, DTE (%), and DTP (%)

Formulation and route of administration	Brain/ blood ratio at 0.5 h	DTI	DTE (%)	DTP (%)
HPL-SLNs i.n.	1.66	5.39	539.31	87.22
HPL-Sol. i.n.	0.079	2.33	233.47	56.17
HPL-Sol. i.v.	0.018	-	-	-

Biodistribution study

Biodistribution studies for both HPL-SLNs and HPL-Sol were performed and observed in different organs of interest and concentration was estimated at different time intervals (0.5, 1, 2, 4, 8, and 24 h) after intranasal administration (Figure 6 & 7).
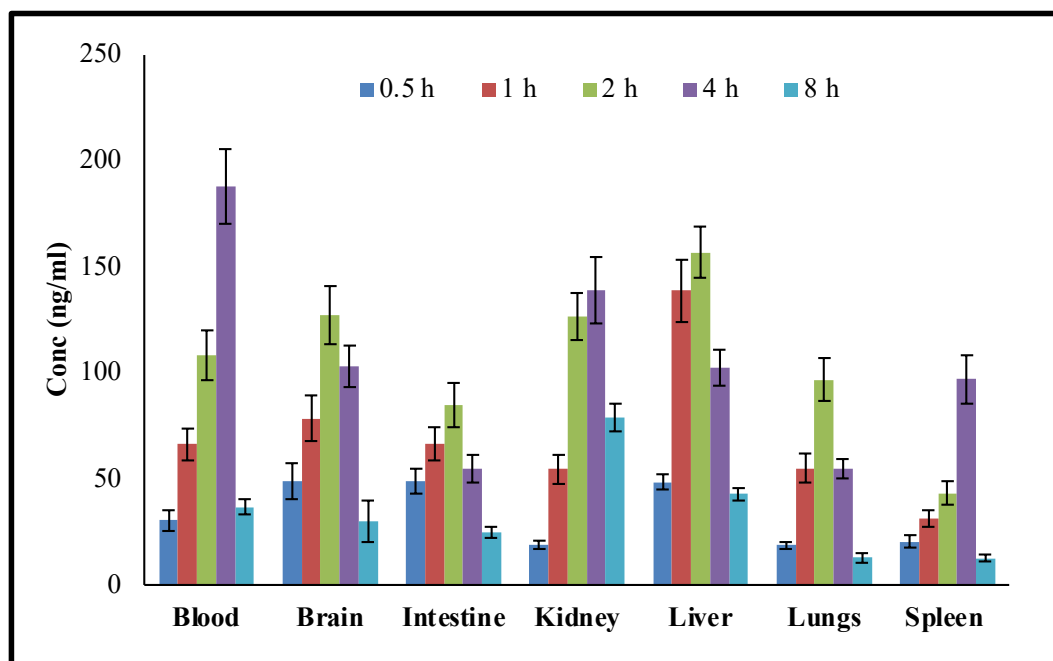
FIGURE 6 - Biodistribution of HPL in Organ of Interest with HPL- SLNs (i.n.).
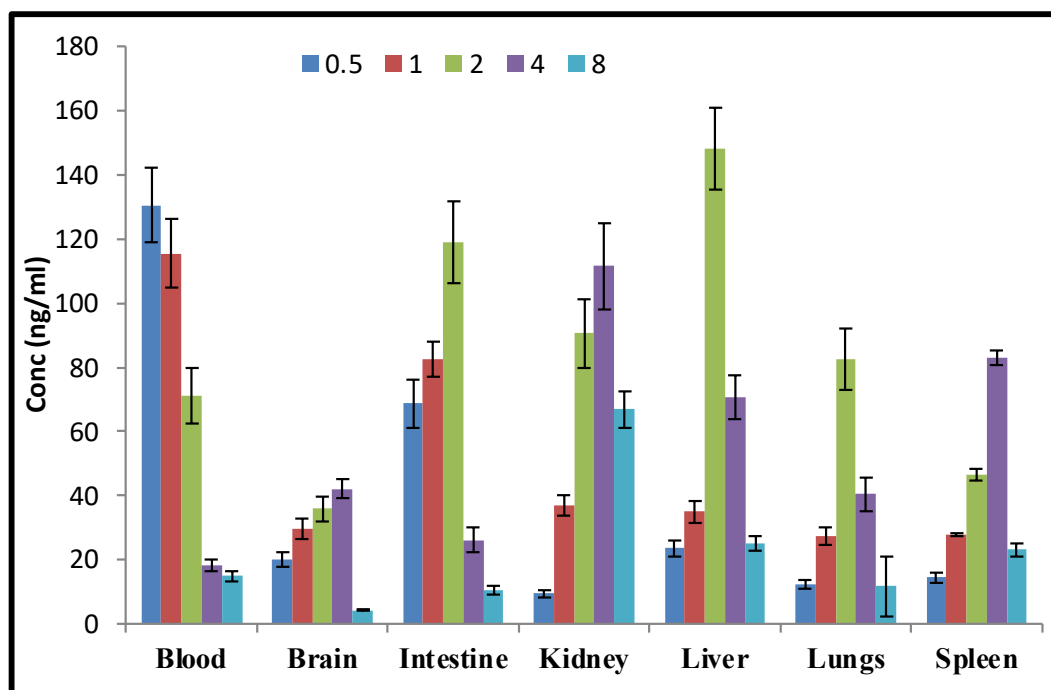
FIGURE 7 - Biodistribution of HPL in Organ of Interest with HPL-Sol (i.n.).

Effect of formulation (HPL-SLNs) on nose-to-brain delivery of HPL: At all time points, significantly higher concentration ($P < 0.01$) of the drug was observed following i.n. administration of HPL-SLNs as compared to a positive control (HPL- Sol. i.n.) which might be due to:

(a) Rapid clearance of the administered HPL-Sol from the nasal cavity by the mucociliary clearance mechanism

(b) By the active efflux transporter pumps at the apical membrane surface (P-gp)

(c) Enzymatic degradation in the olfactory epithelium

SLNs protect the drug from the above mention mechanism and improve the nose to brain delivery. They can protect the encapsulated drug from biological and/or chemical degradation and extracellular transport by P-gp efflux proteins. Moreover, the occlusive nature of lipid provides better nasal retention and hence improves the nasal retention time of SLNs (Singh, Saraf, Saraf, 2012).

Surfactant like Tween 80 was used for the preparation of SLNs and reported to improve brain delivery of nanoparticles by (i) Solubilization of endothelial cell membrane lipids and membrane fluidization (Yasir *et al.,* 2018) (ii) Through the temporary opening of inulin spaces (Gastaldi *et al*., 2014) (iii) Endocytosis of nanoparticles (Yasir *et al.,* 2018), and (iv) Inhibition of efflux system, especially P-gp present on the intranasal membrane (Wang, Jiang, Lu, 2003; Abdelbary, Tadros, 2013).

Effect of formulation (HPL-SLNs) on biodistribution of HPL: Biodistribution studies publicized more localization in kidney, spleen, and liver for HPL-SLNs as compared to HPL sol. The higher level of intranasal HPL-SLNs in different organs might be due to the lipophilic nature of nanoparticulate and their nanosize, enhancement of nasal permeation due to surfactant, preventing from the degrading environment in the nasal pathway (Yasir *et al.,* 2018). Besides, drug-loaded SLNs approached to different organs of the body by different mechanisms. The accumulation in the liver and the spleen is generally ascribed to uptake by the reticuloendothelial system (RES) like macrophage cells (Dobrovolskaia *et al.,* 2008), whereas the presence of lipid nanoparticles in the lungs may be the outcomes of agglomeration caused by the adsorption of plasma

proteins (Singh, Saraf, Saraf, 2012). However, the higher uptake of HPL-SLNs by RES organs may be based on the fact that GMS containing nanoparticles exhibited higher uptake by the RES organs as previously reported by Pandey, Sharma, Khuller (2005).

CONCLUSION

HPL loaded SLNs having nanoscale particle size were developed successfully and evaluated for *in-vitro* & *in-vivo* parameters. All the parameters like particle size, zeta potential, PDI, entrapment efficiency were found to be in an acceptable range. DSC study revealed that the drug was crystalline in pure form and transformed into amorphous form as got entrapped in SLNs. *In-vitro* release study concluded that optimized HPL-SLN formulation exhibited more sustained release as compared to HPL-Sol. Pharmacokinetic and brain targeting studies in rats concluded a considerably high concentration of drug in the brain upon i.n. administration of drug-loaded as compared HPL-Sol. The results of biodistribution studies were in line with the results of pharmacokinetic studies and indicated brain targeting efficiency of developed SLNs formulations. Stability studies disclosed no significant change in the particle size, zeta potential, and entrapment efficiency at 4±2 °C (refrigerator) and 25±2 °C /60 ±5% RH up to six months. The shelf life of optimized formulation was found to be 2.79 years. Hence, it could be concluded that SLNs would be a potential and better carrier for the delivery of HPL to the brain via i.n. route as compared to the drug solution administered intranasally and intravenously.

CONFLICTS OF INTEREST

The authors declare that they have no conflicts of interest.

ACKNOWLEDGMENT

REFERENCES

Abdelbary GA, Tadros MI, Brain targeting of olanzapine via intranasal delivery of core shell difunctional block copolymer mixed nanomicellar carriers: *In vitro* characterization, *ex vivo* estimation of nasal toxicity and *in vivo* biodistribution studies. Int J Pharm. 2013;452(2):300– 310.

Alam T, Pandit J, Vohora D, Aqil M, Ali A, Sultana Y. Optimization of nanostructured lipid carriers of lamotrigine for brain delivery: In vitro characterization and in vivo efficacy in epilepsy. Expert Opin Drug Deliv. 2015;12(2)181–94.

Basha SK, Dhandayuthabani R, Muzammil MS, Kumari VS. Solid lipid nanoparticles for oral drug delivery. Mater Today Proc. 2021;36(2):313-324.

Brasnjevic I, Steinbusch C. Schmitz P, Martinez M. Delivery of peptide and protein drugs over the blood-brain barrier. Prog Neurobiol. 2009;87(4):212–251.

Brincat JV, Macleod AD. Haloperidol in palliative care. Palliat Med. 2004;18(3):195-201.

Budhian A, Siegel SJ, Winey KI. Haloperidol-loaded PLGA nanoparticles: systematic study of particle size and drug content. Int J Pharm. 2007;336(2):367–75.

Bunjes H, Unruh T. Characterization of lipid nanoparticles by differential scanning calorimetry, x-ray and neutron scattering. Adv Drug Deliv Rev. 2007;59(6):379-02.

Chadha R, Bhandari S. Drug excipient compatibility screening—role of thermo analytical and spectroscopic techniques. J Pharm Biomed Anal. 2014;87:82-97.

Chang WH, Lam YWF, Jann MW, Chen H. Pharmacokinetics of haloperidol and reduced haloperidol in chinese schizophrenic patients after intravenous and oral administration of haloperidol. Psychopharmacology. 1992;106(4):517-22.

Chen DB, Yang TZ, Zhang O. *In vitro* and *in vivo study* of two types of long-circulating solid lipid nanoparticles containing paclitaxel. Chem Pharm Bull. 2001;49(11):1444-7.

Dobrovolskaia MA, Aggarwal P, Hall JB, McNeil SE. Preclinical studies to understand nanoparticle interaction with the immune system and its potential effects on nanoparticle biodistribution. Mol Pharm. 2008;5(4):487–495.

Forsman AO. Individual variability in response to haloperidol. Proc R Soc Med. 1976;69(1):9-13.

Fricker G, Kromp T, Wendel A, Blume A., Zirkel J, Rebmann H, et al. Phospholipids and lipidbased formulations in oral drug delivery. Pharm Res. 2010;27(8):1469–86.

Gastaldi L, Battaglia L, Peira E, Chirio D, Muntoni E, Muntoni L, et al. Solid lipid nanoparticles as vehicles of drugs to the brain: Current state of the art. Eur J Pharm Biopharm. 2014;87(3):433–44.

Gidwani B, Vyas A. Preparation, characterization, and optimization of altretamine-loaded solid lipid nanoparticles using Box-Behnken design and response surface methodology. Artif Cells Nanomed Biotechnol. 2016;44(2):571–80.

Haque S, Md S, Sahni JK, Ali J, Baboota S. Development and evaluation of brain targeted intranasal alginate nanoparticles for treatment of depression. J Psychiatr Res. 2014;48(1):1–12.

Higuchi T. Mechanism of sustained action medication: theoretical analysis of rate release of solid drug. J Pharm Sci. 1961;50:74-9.

International Conference On Harmonisation of Technical Requirements For Registration of Pharmaceuticals For Human Use, ICH Harmonised Tripartite Guideline: Stability Testing of New Drug Substances and Products, ICH Q1A-R2, 2003.

Jain R, Nabar S, Dandekar P. Micellar nanocarriers: potentialnose-to-brain delivery of zolmitriptan as novel migraine therapy. Pharm Res. 2010;27(4):655–664.

Jain T, Bhandari A, Ram V, Sharma S, Chaudhary RK, Parakh M. High performance liquid chromatographic method with diode array detection for quantification of haloperidol levels in schizophrenic patients during Routine clinical practice. J Bioanal Biomed. 2011;3(1):8-12.

Jann MW, Kennedy WK. Safety and Tolerability of Antipsychotics. In Spina E,Trifirò G, (Eds.). Pharmacovigilance in Psychiatry. Springer International Publishing, Cham, 2016. PP. 167-189.

Jores K, Mehnert W, Drechsler M. Investigations on the structure of solid lipid nanoparticles (SLN) and oil-loaded solid lipid nanoparticles by photon correlation spectroscopy, field-flow fractionation and transmission electron microscopy. J Control Release. 2004;95(2):217–27.

Kanazawa, T, Taki H, Tanaka K, Takashima Y, Okada H. Cell-penetratingpeptide-modified block copolymer micelles promote direct brain delivery via intranasal administration. Pharm Res. 2011;28(9):2130–9.

Korsmeyer RW, Gurny R., Doelker E, Buri P, Pappas NA. Mechanism of solute release from porous hydrophilic polymers. Int J Pharm. 1961;15(2):25-35.

Kumar M, Misra A, Babbar AK, Mishra AK, Mishra P, Pathak K. Intranasal nanoemulsion based brain targeting

drug delivery system of risperidone. Int J Pharm. 2008;358(1):285-91.

Pandey R, Sharma S, Khuller GK. Oral solid lipid nanoparticle-based antitubercular chemotherapy. Tuberculosis. 2005;85(5):415–20.

Pandita D, Ahuja A, Velpandian T, Lather V, Dutta T, Khar R.K. Characterization and in vitro assessment of paclitaxel loaded lipid nanoparticles formulated using modified solvent injection technique. Pharmazie. 2009;64(5):301–10.

Patel MN, Lakkadwala S, Majrad MS, Injeti ER, Gollmer SM, Shah ZA, et al. Characterization and Evaluation of 5-Fluorouracil-Loaded Solid Lipid Nanoparticles Prepared via a Temperature-Modulated Solidification Technique. Ageing Int. 2014;15(6):1498–508.

Schwarz C, Mehnert W, Lucks JS, Muller RH. Solid lipid nanoparticles for controlled drug delivery- I. production, characterization and sterilization. J Control Release. 1994;30(1):83–96.

Settle EC, Ayd FJ. Haloperidol: a quarter century of experience. J Clin Psychiatry. 1983;44(12):440-48.

Shah AK, Date AA, Joshi MD, Patravale VB. Solid lipid nanoparticles of tretinoin: potential in topical delivery. Int J Pharm. 2007;345(2):163-71.

Shah. B, Khunt, D, Bhatt H, Misra M, Padh H. Application of quality by design approach for intranasal delivery of rivastigmine loaded solid lipid nanoparticles: Effect on formulation and characterization parameters. Eur J Pharm Sci. 2015;78:54-66.

Singh AP, Saraf SK, Saraf SA. SLN approach for nose-to-brain delivery of alprazolam. Drug Deliv Transl Res. 2012;2(6):498-507.

Soutto EB, Wising SA, Barbosa CM, Muller RH. Development of a controlled released formulation based on SLN and NLC for the topical clotrimazole delivery. Int J Pharm. 2004;278(2):71-7.

Trotta M, Debernardi F, Caputo O. Preparation of solid lipid nanoparticles by a solvent emulsification diffusion technique. Int J Pharm. 2003;257(2):153-60.

Varshosaz J, Tabbakhian M, Mohammadi MY. Formulation and optimization of solid lipid nanoparticles of buspirone HCl for enhancement of its oral bioavailability. J Liposome Res. 2010;20(4):286-96.

Wang F, Jiang X, Lu W. Profiles of methotrexate in blood and CSF following intranasal and intravenous administration to rats. Int J Pharm. 2003;263(2):1-7.

Wang W, Wang C, Zhang Y, Fu H, Gao, Zhang R. Preparation and characterization of solid lipid nanoparticles loaded with

Mohd Yasir, Iti Chauhan, Ameeduzzafar Zafar, Madhu Verma, Nabil K Alruwaili, K. M Noorulla, Alok Pratap Singh, Abdurrazak Jemal Tura

salmon calcitonin phospholipid complex. J Drug Deliv Sci Tec. 2019;52:838-45.

Wong HL, Wu XY, Bendayan R. Nanotechnological advances for the delivery of CNS therapeutics, Adv Drug Deliv Rev. 2012;64(7):686-700.

Yasir M, Sara UVS, Chauhan I, Gaur PK, Singh AP, Puri D, et al. Solid lipid nanoparticles fornose to brain delivery of donepezil: formulation, optimization by Box–Behnken design,in vitro and in vivo evaluation. Artif Cells, Nanomed Biotechnol. 2018;46(8):1838-51.

Yasir M, Sara UVS. Development and validation of UV spectrophotometric method for the estimation of haloperidol. Br J Pharm Res. 2014;4(11):1407-15.

Zhang QZ, Jiang XG, Jiang WM, LU W, SU LN, SHI ZQ. Preparation of nimodipine-loaded microemulsion for intranasal delivery and evaluation on the targeting efficiency to the brain. Int J Pharm. 2004;275(2):85–96.